

UNIVERSITY OF NEVADA, RENO

A continuous method for measurement of pH and acidity in ice cores

A thesis submitted in partial fulfillment of
the requirements for the degree of Master of
Science in Hydrology

by
Daniel R. Pasteris

Dr. Joseph R. McConnell
Thesis Advisor

May 2009



University of Nevada, Reno
Statewide • Worldwide

THE GRADUATE SCHOOL

We recommend that the thesis
prepared under our supervision by

DANIEL R. PASTERIS

entitled

A Continuous Method for the Measurement of pH and Acidity in Ice Cores

be accepted in partial fulfillment of the
requirements for the degree of

MASTER OF SCIENCE

Joseph R. McConnell, Ph. D., Advisor

P. Ross Edwards, Ph. D., Committee Member

Gina Tempel, Ph. D., Graduate School Representative

Marsha H. Read, Ph. D., Associate Dean, Graduate School

May, 2009

Abstract

A continuous direct measurement technique has been developed for the accurate determination of pH and acidity in ice cores at monthly to seasonal resolution. A small flow-through bubbling chamber is employed for sample equilibration with a known concentration of carbon dioxide and the measurement is made with a traditional glass pH electrode. The technique provides both high resolution accuracy and efficiency that cannot be found with the existing techniques of electrical conductivity measurement (ECM), Gran titration, or discrete pH measurement. A 63-year acidity record from the Humboldt North ice core in northwest Greenland is presented and compared to the major ion data from the ice core to determine the relative importance of the species that are responsible for the acidity. Sulfuric acid (H_2SO_4) followed by nitric acid (HNO_3) were found to be the primary acid components, with hydrochloric acid (HCl) and organic acids (HOrg) also contributing. Ammonia (NH_3) was the primary basic component followed closely by carbonate (CO_3). Acidity ranges from 1 to 11 μM (pH 5.5 – 4.9) with a distinct annual peak in late winter-early spring. Trends in the acid and base species are examined and show that recent decreases in H_2SO_4 have been partially compensated for by increases in HNO_3 and HCl . The correlation between HNO_3 and HCl supports an existing body of aerosol data showing HCl production by acid displacement on sea salt aerosols is greater in the presence of HNO_3 than other acids.

Table of Contents

Abstract.....	i
Introduction.....	1
Background.....	2
Methodology.....	4
Theory.....	5
Procedure.....	7
Results.....	15
Discussion.....	16
Chemical Species Driving Acidity.....	16
Excess Chloride.....	24
Recent Trends.....	26
Summary and Future Research.....	29
References.....	32

List of Tables and Figures

Table 1	Estimated formate events.....	17
Figure 1	Conductivity measurement comparison.....	12
Figure 2	Calibration curve.....	14
Figure 3	Measured pH and acidity profiles.....	15
Figure 4.	Modeled acidity comparisons.	22
Figure 5	Measured acidity vs. $A_{CY_{Relev}}$ modeled scatterplot.....	23
Figure 6	$A_{CY_{Relev}}$ and measured acidity comparison.....	23
Figure 7	Excess chloride acidity spike.....	25
Figure 8	Long term trends in relevant species.	27
Figure 9	Acidity comparison with Alert aerosol data	29

Introduction

The pH of precipitation has drawn considerable attention since the 1970s with the realization that human induced acid rain can negatively affect fisheries, forest ecosystems and human structures (*Oden et al.*, 1968; *Likens et al.*, 1979, 1996; *Johnson et al.*, 1982; *Drever and Hurcomb*, 1986; *Schindler et al.*, 1988). Acid rain or snow is defined as precipitation with a pH below approximately 5.6, which is the pH of pure water in equilibrium with the present day atmospheric concentration of carbon dioxide. A precipitation sample is also a useful proxy for atmospheric aerosol and gas phase chemistry, where pH plays an important role in processes such as aerosol speciation, persistence of acidic sulfate aerosol and associated radiative forcing, the uptake of acids and bases by aerosol particles, and the presence of cloud condensation nuclei (*Jang et al.*, 2002; *Wolff et al.*, 1997a; *Maupetit and Delmas*, 1994; *Girard et al.*, 2005).

Ice cores provide a valuable record of precipitation chemistry dating back hundreds of thousands of years that can be used to reconstruct the atmospheric conditions of past climates as well as the extent of human influence in present times. The analysis of ice cores by continuous melting and real-time analysis by inductively coupled mass spectrometer (ICP-MS) and absorption and fluorimetric spectroscopy has allowed for high resolution records of major ions and trace metals at extremely low detection limits (*McConnell et al.*, 2002). A continuous flow technique has now been developed for the accurate and high resolution measurement of pH and acidity in ice cores.

Background

The pH, or negative log of the hydrogen ion activity, $-\log_{10}\{H^+\}$, of a melted ice core sample is the result of strong acids and bases and the equilibrium dissociation of any weak acids or bases that may be present. The acids and bases that are often of greatest influence are carbonic acid (H_2CO_3), sulfuric acid (H_2SO_4), nitric acid (HNO_3), calcium carbonate ($CaCO_3$), and ammonia gas (NH_3). Some additional influence may result from minor amounts of hydrochloric acid (HCl) and weak organic acids such as formic acid ($HCOOH$) and acetic acid (CH_3COOH).

Carbon dioxide forms the weak acid carbonic acid (H_2CO_3) when dissolved in water, which increases the hydrogen ion activity, but because carbon dioxide is present in all precipitation and surface water samples exposed to the atmosphere, it is often more useful to consider the acidity (Acy) or alkalinity (Alk = negative H-Acy) of a precipitation sample. These measures give the net concentration of acid or base, respectively, relative to a reference state of water in equilibrium with carbon dioxide. Our measure of acidity is that of carbonate acidity, defined with an H_2CO_3 - H_2O reference state by the equation

$$Acy = [H^+] - [HCO_3^-] - 2[CO_3^{2-}] - [OH^-] \quad (1)$$

Any H^+ contribution from dissociated H_2CO_3 is matched by the presence of HCO_3^- , or CO_3^{2-} , and therefore does not contribute to the acidity value. The acidity can be operationally defined as the amount of base required to bring the pH of an acidic solution up to the H_2CO_3 endpoint, which is approximately 5.6 for water at $25^\circ C$ in equilibrium with a CO_2 concentration of 385 ppm at a pressure of 1 atm.

Existing methods of obtaining pH and acidity data from ice cores are pH measurement of CO₂ equilibrated discrete samples, Gran titration of discrete samples, and electrical conductivity measurements (ECM) of still frozen ice cores and [Hammer, 1983; Legrand *et al.*, 1982; Simoes and Zagorodnov, 2000]. A simple titration of discrete ice core samples is not possible because the method is not precise enough to measure the low levels of acidity found in ice cores.

pH measurements of discrete samples must be equilibrated with a known concentration of carbon dioxide to be converted to an acidity value (see Methods section). The CO₂ concentration in an occupied laboratory will vary depending on the number of people in the room and the quality of the fresh air source; therefore a supply tank should be used for measurements with precision greater than 1 μM. The discrete method is essentially the same as the continuous method described here, except that measurement of discrete samples is very time consuming and generally results in decreased temporal resolution.

Gran titration is a discrete sample technique that avoids the carbon dioxide problem by performing pH measurements below pH 4.5, where no carbonic acid dissociation occurs and the carbon dioxide concentration is irrelevant. The technique has seen limited application (Walker *et al.*, 2003; Isaksson, 2001; Ginot *et al.*, 2001) typically on a limited number of discrete samples. While potentially very precise, the method suffers from the time efficiency issues of a discrete method, and is somewhat complicated to perform at an adequate level of precision due to the small volume of dilute sample being titrated and the very stable temperature and pH electrode conditions that must be maintained.

ECM measures the direct current electrical conductivity of frozen ice core samples, which is driven exclusively by the hydrogen ion concentration of the ice. The method provides a quick, non-destructive, semi-quantitative measure of acidity that has been useful in assessing climate variability at high temporal resolution (*Taylor et al.*, 1993, 2003; *Wolff et al.*, 1997a). The accuracy of the technique is limited, however, due to a fair amount of uncertainty in the calibration. This uncertainty arises due to error in the acidity measurements used in the calibration, potential variability in the ECM measurements due to core quality and operating conditions, and an apparent differential response between the acid species H_2SO_4 , HNO_3 , and HCl (*Wolff et al.*, 1997b, and references therein). Also, because the conductivity goes to zero as the acidity goes to zero, the ECM method has been unable to serve as a quantitative measure of alkalinity (*Moore et al.*, 1994). Alkaline ice exists in both hemispheres during cold climate periods when dust concentrations are high, such as during most of the Wisconsin glaciation (*Wolff et al.*, 1997a).

Methodology

The acidity record produced in this analysis is from a 21 meter long ice core collected in Summer, 1995 at the Humboldt North site in northwest Greenland ($78^{\circ}45'06''$ N, $56^{\circ}49'56''$ W) at an elevation of 1,905 meters (*Anklin et al.*, 1998). Sticks measuring approximately 1 meter by 3.5 cm by 3.5 cm were continuously melted at a rate of approximately 6 cm/min in our continuous ice core melting system. Acidity was one of many simultaneous online, continuous measurements made on the ice core. Additional species include nitrate and chloride, measured by absorption spectroscopy; ammonium by

flourimetric spectroscopy; and soluble sulfur, sodium, and calcium by ICP-MS. The ice core record covers the time period from 1932 to 1994, and was dated with an accuracy of ± 1 year by counting the distinct annual cycles of analyte concentrations.

Theory

The method presented in this paper consists of accurate pH measurements of samples in equilibrium with a known partial pressure of carbon dioxide, allowing for calculation of acidity by Equation 1. The H^+ and OH^- terms in the right-hand side of Equation 1 are determined directly from the pH measurement, while the HCO_3^- and CO_3^{2-} are calculated from the total concentration of carbonate species (C_T) and the ionization fractions of H_2CO_3 , which depend only on P_{CO_2} and $[H^+]$. The Henry's Law constant for CO_2 (K_H), the dissociation constant of water (K_w), and the first and second dissociation constants of H_2CO_3 (K_1 and K_2) are also required for the calculation. The equations used to solve for acidity are presented below (Stumm and Morgan, 1996), where Equation 2 is simply Equation 1 written in terms of H^+ , P_{CO_2} , the ionization fractions (α_0 , α_1 , α_2) and the necessary equilibrium constants.

$$Acy = [H^+] - \frac{K_H P_{CO_2}}{\alpha_0} (\alpha_1 + 2\alpha_2) - \frac{K_w}{[H^+]} \quad (2)$$

$$C_T = \text{total carbonate} = \frac{K_H P_{CO_2}}{\alpha_0} \quad (3)$$

$$\alpha_0 = H_2CO_3 \text{ ionization fraction} = \left(1 + \frac{K_1}{[H^+]} + \frac{K_1 K_2}{[H^+]^2} \right)^{-1} \quad (4)$$

$$\alpha_1 = \text{HCO}_3^- \text{ ionization fraction} = \left(\frac{[\text{H}^+]}{K_1} + 1 + \frac{K_2}{[\text{H}^+]} \right)^{-1} \quad (5)$$

$$\alpha_2 = \text{CO}_3^{2-} \text{ ionization fraction} = \left(\frac{[\text{H}^+]^2}{K_1 K_2} + \frac{[\text{H}^+]}{K_2} + 1 \right)^{-1} \quad (6)$$

The accuracy of the acidity value calculated by Equation 1 (same as Equation 2) relies on the assumption that concentrations of weak acids, most notably organic acids, are insignificant. The presence of a weak acid with a pK_a value close to 5.6 would buffer the pH during an acidity titration, which would necessitate the addition of slightly more base to bring the solution to the bicarbonate endpoint of pH 5.6. In other words, the presence of weak acids can cause Equation 1 to underestimate acidity value obtained by titration. Such a titration is unable to accurately measure acidity at the low values found in ice cores and most precipitation samples, but it is the operational definition of carbonate acidity and is used here for the purpose of explanation.

The expected magnitude of this problem has been investigated using mean concentrations of organic acid anions from an ice core in Summit, Greenland (*Legrand and De Angelis, 1996*). The reported mean concentrations of organic acid anions formate, acetate, glycolate, and oxalate during preindustrial, industrial, biomass burning, and volcanic events were input into the aqueous chemical equilibrium model MINTEQA2. Simulated titrations were performed to assess the error in the acidity calculated by Equation 1 that would result from the buffering effect of the organic acids. Assuming the concentrations of organic acid anions are similar between Summit, Greenland and the Humboldt North site, the mean negative bias will be less than 1%

during the majority of the record and up to 3% during occasional biomass burning events, marked by high ammonium and formate concentrations.

Formate concentrations during biomass burning events in our Humboldt North ice core were estimated using the measured ammonium concentration and the highly correlated relationship between ammonium and formate reported from Summit, Greenland (*Legrand and De Angelis, 1996*). The estimated formate values are of the same magnitude as the peaks in the reported Summit data and are consistent with a maximum error of 3% during the highest biomass burning events observed in the Humboldt North record. This error could be accounted for by adding the estimated concentration of undissociated formic acid to acidity obtained by Equation 1, thereby changing the reference state of the acidity calculation to $\text{H}_2\text{CO}_3\text{--H}_2\text{O--COOH}^-$. This is perhaps the most rigorous method of handling the organic acids, however there are no direct measurements of formate in our analysis, so we will leave the reference state as presented in Equation 1 and accept a very small and very infrequent source of error.

Procedure

The continuous sample stream used in the analysis is generated by melting ice core sticks in succession from the bottom to the top of the ice core. As the melted sample is generated, a portion from the uncontaminated center of the stick is diverted to a glass pH electrode placed in a plastic flow cell. Potassium chloride solution is added at a constant proportion to obtain a constant sample ionic strength of 0.01 μmol . The elevated ionic strength serves to stabilize the electrode junction potential and decreases the response time by increasing the electrical conductivity of the sample solution.

The acidic influence of carbon dioxide is problematic when attempting to measure ice core sample pH in a continuous flow configuration. Uncertainty and potential variability in the concentration of carbon dioxide in the sample stream at the pH electrode arises because carbon dioxide is essentially excluded from the snow grains when they form (*Killawee et al.*, 1998; *Neftel et al.*, 1983), leading to ice cores containing very little carbon dioxide in the ice and paleoatmospheric concentrations of carbon dioxide in the pore spaces. During analysis, the newly melted sample therefore begins with very little dissolved carbon dioxide, but instantly begins to dissolve it according to Henry's Law.

While the sample travels from the ice melter to the pH electrode in our sampling configuration, it is exposed to a mixture of ice core pore air and laboratory air for less than two minutes. A high pH baseline of 5.8 to 5.9 for continuous ice core measurements performed without the use of any equilibrium device indicates that the sample is not reaching equilibrium with the mixture of air it has been exposed to during analysis, because a clean water sample in equilibrium with atmospheric levels of carbon dioxide has a pH of approximately 5.6. Because the level of CO₂ equilibrium at the pH probe could vary during a continuous analysis, particularly under the high gradient indicated by the unequilibrated measurements, accurate measurement of pH requires forced equilibrium of the sample with a known concentration of carbon dioxide.

A glass bubbling chamber consisting of a fritted glass tube surrounded by a small glass flow cell has been assembled for the purpose of equilibrating the sample stream. Nitrogen gas containing 385ppm CO₂ is bubbled through the sample as it flows through the bubbling chamber. The cell has a mixing volume of less than 400 μL, which is limited by the volume of the supplied air, and allows for rapid equilibration with minimal

sample dispersion. The typical flow rate through the bubbler is ~2 mL/min, giving a mean residence time of ~12 seconds. In addition to providing pH measurements that are essentially free of uncertainty in the CO₂ content, the constant and known CO₂ concentration allows for acidity to be accurately calculated by Equation 2. Because acidity is independent of CO₂ concentration, it is more appropriate than pH for comparison of measurements performed at different locations or with different CO₂ supply tanks, and will therefore be considered the primary result of this method.

The effectiveness of the bubbling chamber in equilibrating the sample stream is verified by supplying it with deionized water at various depleted concentrations of carbon dioxide and measuring any change in pH that may occur after passing through the bubbler. The degree of carbon dioxide depletion in the deionized water is easily determined by measuring its pH before any equilibration attempt has been made, and is expressed here as the atmospheric concentration of carbon dioxide with which it would be equilibrated. For example, a sample with a pH of 5.9 would be in equilibrium with an atmospheric CO₂ concentration of 95 ppm, and would be 25% equilibrated with an atmospheric concentration of 385 ppm, while a sample with a pH of 5.8 would be about 39% equilibrated. These experiments show that the bubbler is capable of inducing >99% equilibration for samples that are at least 50% equilibrated upon entering the bubbler, and will induce >95% equilibration for samples entering the bubbler that are greater than 15% equilibrated. Since the ice cores are approximately 25% – 40% equilibrated upon entering the bubbler (pH 5.8 – 5.9), it is presumed that they exit between 95% and 100% equilibrated.

The kinetics of the CO₂ dissolution are limiting the ability of the bubbler to fully equilibrate the sample within the 12 second mean residence time of the sample. The CO₂ gas transfer behaves according to Fick's law of diffusion across a diffusion film at the water-air interface, and is described by the equation:

$$F = \frac{D_{\text{CO}_2}}{z_w} ([\text{CO}_2]_{\text{w}} - [\text{CO}_2]_{\text{w/a}}) \quad (7)$$

F is the molecular flux in units of mol cm⁻² s⁻¹, D_{CO₂} is the molecular diffusion coefficient in units of cm² s⁻¹, and z_w is the diffusion film thickness measured in cm. [CO₂]_w is the depleted concentration of CO₂ in the water and [CO₂]_{w/a} is the fully equilibrated concentration in the water at the water-air interface, each in units of mol/cm³. Approximations of the time to obtain equilibrium can be made using Equation 7 with a well established D_{CO₂} value of 2 x 10⁻⁵ cm² s⁻¹, z_w values within the range of a few micrometers, a bubbler water volume of 0.4 mL, and surface area values within the range of a few cm². The low diffusion film thickness is reasonable for a high turbidity water (*Stumm and Morgan, 1996*), and the surface area values are reasonable estimations for conditions in the bubbling chamber. The volume of water in the bubbler is known from our sample flow measurements. The diffusion calculations indicate that the time required for equilibrium is on the order of 10 – 30 seconds, which is in agreement with our attainment of > 95% equilibrium in approximately 12 seconds of bubbler residence time.

Turbulent mixing within the bubbling chamber increases the molecular flux by increasing the water's surface area and by decreasing the water film thickness, z_w. The flux is greatest when the concentration gradient is largest, resulting in relatively rapid

progress toward 95% equilibration, with slower progress occurring in the final stages of reaching 100% equilibration. Greater equilibration could be obtained with longer sample residence time in the bubbler, however this would be at the expense of decreased resolution due to increased sample mixing. Experiments performed with pre-equilibrated water show that the maximum error due to variable equilibration in the range of 95% and 100% is less than 0.1 μM of acidity when the acidity is less than 4 μM , and is less than 0.05 μM otherwise. Since the loss of resolution is very low when high flow rates are used, error and uncertainty are minimized by retaining the relatively minor $<0.1 \mu\text{M}$ error in acidity due to slightly incomplete equilibration.

Response time of the pH probe is less than 3 seconds per acidity unit and therefore not a factor in the accuracy of the measurement. Uncertainty in the degree of signal smoothing due to mixing in the bubbling chamber and pH flow cells can be assessed by comparing the acidity to the highly correlated electrical conductivity measurement, which is measured prior to the sample entering the bubbling chamber. Figure 1 presents the comparison for a section of Humboldt North ice core. The relative height of the peaks cannot be expected to match perfectly because conductivity depends on other ions in addition to H^+ . The very close similarity in peak width among the two signals indicates that the acidity signal is not being smoothed significantly by the mixing in the low-volume bubble chamber or electrode flow cell.

Signal smoothing, while typically negligible, is expected to occur to a small degree during high-amplitude, high-frequency acidity cycles. These instances will result in a small negative bias during peaks and a small positive bias during troughs. Signal smoothing will not affect the accuracy of multiyear averages or long term trends, since all

of the acidity is still measured. Based on the assessment of the various predicted acidity models presented in the Discussion section, the occasional smoothing bias during individual months of high amplitude events in the Humboldt North ice core is expected to be less than $0.5 \mu\text{M}$ or 10% of the measured signal, whichever is greater. These smoothing bias estimates are specific to the Humboldt North ice core, which is a site with a relatively high amplitude and high frequency acidity signal.

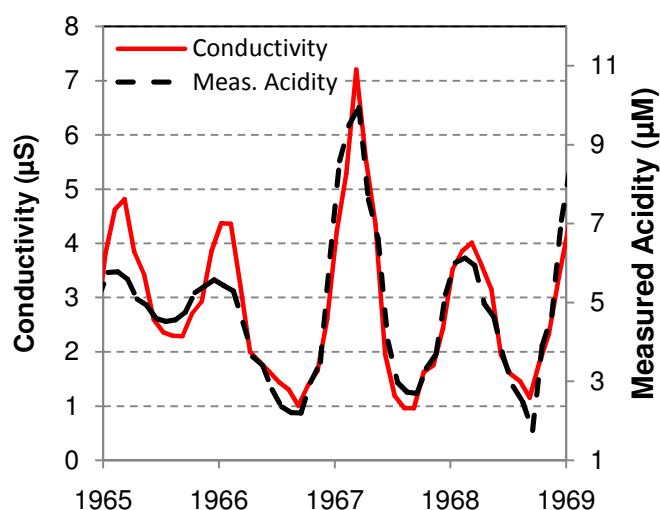


Figure 1 Fast response conductivity measurement compared to acidity measurement, showing an equally fast response with essentially no smoothing due to mixing in the CO_2 bubbling chamber.

Calibration of the pH probe is performed with precisely prepared acidity standards of 0, 5, 10, and $20 \mu\text{M}$ which are pumped through the continuous flow system in the same fashion as the ice core samples. The calculated pH of each acidity standard in equilibrium with the supplied carbon dioxide level is used to obtain the linear pH vs. mV calibration equation (Figure 2). This direct calibration method produces a pH value that measures the true concentration of hydrogen ion ($\text{p}^{\text{c}}\text{H}$), not the activity value that would be measured if the calibration was performed with buffers. This is important

because acidity of a solution is a conservative property that is not affected by changes in ionic strength. Calculation of acidity using H^+ activity in Equation 2 would result in an underestimation of the acidity by a factor of one minus the activity coefficient ($1-\gamma$).

While the activity coefficient can be estimated to be approximately 0.90 in a 0.01 M ionic strength solution, it is preferable to eliminate the uncertainty associated with a correction by performing the calibration with acidity standards. The direct acidity calibration is also beneficial because it minimizes uncertainty associated with other parameters in Equation 2. A buffer calibration, performed with low ionic strength buffers, does provide an accurate measurement of blank water with zero acidity, and is useful for verifying that the acidity of the deionized water used to make the acidity standards is in fact zero.

Figure 2 shows the results of a calibration with acidic and alkaline standards ranging from $-10 \mu\text{M}$ to $20 \mu\text{M}$ acidity, including a blank water measurement of zero acidity.

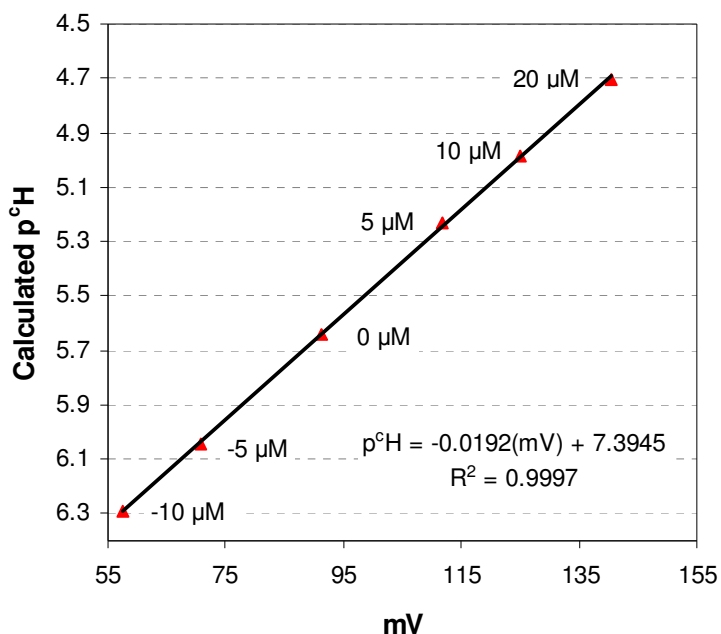


Figure 2 An example calibration curve for converting the measured hydrogen ion electrode mV value to pH. The strong linear fit allows for high accuracy over the full range of measurement. Acidity standards (-10 μM through 20 μM in this example) are prepared by precise dilution of 0.1 M HCl or NaOH. The hydrogen ion electrode response is linear in units of pH, so the pH of each acidity standard with known CO_2 concentration is calculated by solving Equation 2 for H^+ . Subsequent sample measurements are made in units pH, then acidity is calculated using Equation 2. The use of acidity standards that are subject to the same carbon dioxide equilibration conditions and the same addition of 1% KCl is essential for accurate calibration. A calibration with pH buffers will result in error when converting to acidity, because it will calibrate for activity, not concentration.

Overall uncertainty of the technique was estimated with Monte Carlo simulations that account for propagation of all recognized uncertainties in the pH calibration procedure and in the terms appearing in the acidity calculation by Equation 2. The overall uncertainty, expressed as the standard deviation of the error and neglecting occasional short-term bias due to smoothing, is $\pm 0.20 \mu\text{M}$ in the range of 0 to 5 μM acidity, above which it is $\pm 5\%$. The uncertainty is limited by variability of less than 1 percent in the slope of the calibration equation throughout a day of analysis. The

calibration uncertainty represents a combination of experimental error in standard preparation and drift in the slope (slope = mV per pH unit) of the pH electrode.

Results

The profiles of measured acidity and pH are presented in Figure 3.

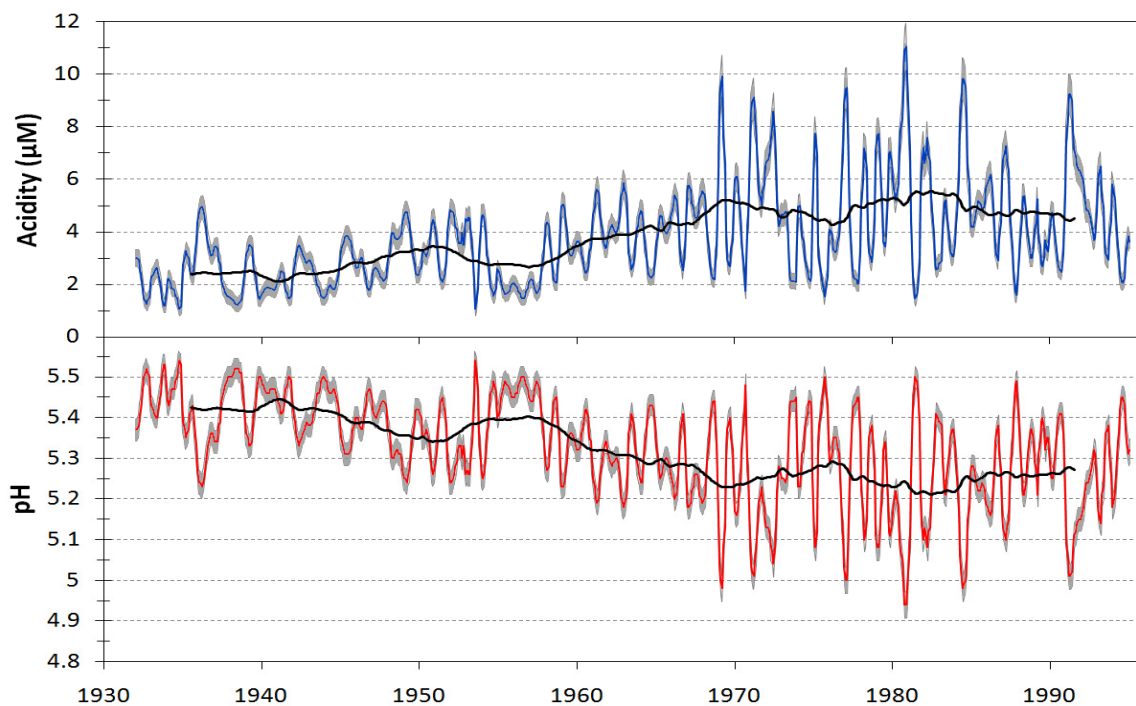


Figure 3 Profiles of acidity and pH as measured in the Humboldt North ice core. Trend line is a 7 year running average and the envelope is the 95% confidence interval.

Prior to 1960s the acidity can be seen to fluctuate between 1 and 5 μM , and beginning around 1960 the values increase to a range between 2 and 11 μM . This period of heightened acidity coincides with the peak of industrial emissions in the northern hemisphere. The 7-year average displays a doubling in average acidity over the time series. A distinct annual cycle is present, with acid peaks occurring in the winter-spring (December to March). This corresponds to the time of greatest atmospheric transport to

the arctic from the populated regions of North America and Eurasia and the occurrence of Arctic Haze (*Barrie, 1986; Klonecki et al, 2003*).

Discussion

Chemical Species Driving Acidity

Acidity can be calculated from the ion balance of a water sample when all significant ions have been accurately measured. An ion balance estimate of acidity provides a rough verification of the continuous acidity measurement, and serves as a starting point for identifying those species that correspond to a direct affect on acidity, referred to herein as acid relevant species.

The ion balance calculation of acidity, in units of equivalents/L, takes the form:

$$[\text{Acy}_{\text{IonBal}}] = [\text{H}^+] - [\text{HCO}_3^-] = [\text{SO}_4^{2-}] + [\text{NO}_3^-] + [\text{Cl}^-] + [\text{Org}^-] - [\text{NH}_4^+] - [\text{Ca}^{2+}] - [\text{Na}^+] - [\text{Mg}^{2+}] - [\text{K}^+] \quad (8)$$

Our ice core analysis did not include organic acid anions (Org^-) or potassium, which necessitates the use of estimated values for these generally minor components. Additionally, measured total sulfur was used to approximate the sulfate concentration. Organic acid anion concentration was approximated solely by an estimated formate concentration, computed according the highly correlated relationship with ammonium found in Summit, Greenland (*Legrand and De Angelis, 1996*). The reported regression equation is $[\text{Formate}] = 0.95[\text{NH}_4^+] - 0.9$, with units in $\mu\text{eq/L}$. The regression only applies when the ammonium concentration is greater than $1.0 \mu\text{M}$, which occurs during infrequent events of strong biomass burning influence. The presence of formate during high ammonium events is supported in our Humboldt North record by a significant

negative ion balance and an April through October timing of all events, as demonstrated in Table 1. Potassium concentration was approximated using the sodium concentration to estimate sea salt potassium. Since both formate and potassium are generally very minor constituents, these estimations are adequate for a first approximation of acidity using the ion balance approach. The $Ac_{Y_{IonBal}}$ model performs well, with a correlation coefficient of 0.922 when compared to the measured acidity. A representative segment of the resulting time series is presented in Figure 4, which shows the close correlation with the measured acidity. Portions of the time series where the $Ac_{Y_{IonBal}}$ model does not match the measured data are due to cations or anions that are missing from the analysis or from errors in approximating or measuring chemical species included in the calculation.

Year	Month	Formate	Neg. Ion Bal
1935	Jul	1.1	1.3
1937	Sept	2.5	2.6
1943	Oct	4.2	3.6
1951	Apr	4.4	4.1
1956	Jul	1.2	1.1
1971	Aug	2.9	1.6
1974	May	2.4	2.7

Table 1 The seven events during the 63 year record with estimated formate concentrations greater than 1.0 are presented along with the timing of the event and computed negative ion balance during those time periods. Formate was estimated by the formula $[Formate] = 0.95[NH_4^+] - 0.9$ (Legrand and De Angelis, 1996) and applied when the concentration of ammonium was greater than 1 μM . All of the events occur between April and October, and except for the 1971 event, the negative ion balance and formate concentrations are in good agreement.

In an effort to improve the fit and eliminate some of the uncertainty in the Acy_{IonBal} calculation, species or fractions of species that are presumed to have no affect on the acidity of the ice core were removed from Equation 8. Those species removed were sea salt sulfate (ss SO_4^{2-}), sea salt chloride (ss Cl^-), sea salt calcium (ss Ca), total sodium, total magnesium, and total estimated potassium. The resulting equation for acidity computed using only acid relevant species, in units of equivalents/L is:

$$[Acy_{Relev}] = [nss SO_4^{2-}] + [NO_3^-] + [excess Cl^-] - [excess NH_4^+] - [nss Ca^{2+}] \quad (9)$$

The Acy_{Relev} model fits slightly better than the ion balance model, with a correlation coefficient of 0.929, demonstrating that the non-acid relevant species can be removed from the model without detriment, and that some improvement can be gained from eliminating the uncertainty associated with those species that are removed. The scatter plot of measured versus modeled data (Figure 5) demonstrates the near one-to-one correlation, while the complete profile (Figure 6) reveals a slight tendency to overestimate the high measured values and underestimate the low values. All of the species in Equation 9 are considered to be a proxy for an acid or base species, so Acy_{Relev} represents the sum of sulfuric acid, nitric acid and hydrochloric acid, minus ammonia and calcium carbonate.

Non sea salt sulfate and calcium used in the Acy_{Relev} model were calculated using the sodium concentration and the standard seawater ratios. Excess chloride (also non sea salt Cl) is that which is present in excess of the sea salt ratio and is presumed to be HCl. Negative excess chloride occurs during a few instances of high sea salt concentration in the record. The measured acidity data does not show any decline during these periods

and therefore does not support the possibility that these events represent sea salt dechlorination with loss of acid from the system as HCl. Reemission of HCl occurs in low accumulation sites receiving less than 4 cm water equivalent per year in Antarctica (*Rothlisberger et al.*, 2003), but is not generally found in Greenland, where accumulation rates are higher (*Legrand and Mayewski*, 1997). The average accumulation rate of 14 cm of water equivalent per year at the Humboldt site is therefore expected to be too high for significant reemission of HCl. Because they do not appear to represent acid loss, the negative values of excess chloride are not included in the $A_{cy_{Relev}}$ model and are assumed to be the result of excess sodium or the small amount of uncertainty (<5%) in the magnitude of the chloride data. The excess ammonium term in Equation 9 represents ammonia that has not been neutralized by formic acid. Inclusion of non sea salt magnesium, which might be thought to correspond to additions of carbonate base to the system, provides no improvement to the relevant species model, or the regression model discussed below, and was not included.

It is worth noting that nitrate and ammonium that enter the system as acid neutral NH_4NO_3 , and calcium and sulfate that enter the system as acid neutral $CaSO_4$ will cancel each other out in Equation 9. Therefore, for the purposes of modeling the acidity time series, it is not necessary to account for the portion of each species derived from these non acidic sources. A minor misrepresentation of acid contribution occurs due to the small amounts of the methanesulfonic acid (MSA) that are being lumped into the sulfate measurement. MSA is a monoprotic acid, so the acidity due to sulfur species will be overrepresented by the assumption that all of the measured total sulfur is derived from diprotic sulfuric acid. It is estimated that MSA accounts for an average of less than 3%

of the sulfur acidity since 1930, based on mean $MSA/(MSA + nssSO_4^{2-})$ ratios reported from Svalbard and Summit, Greenland (*Legrand et al.*, 1997, *Isaksson et al.*, 2001). The MSA contribution will vary seasonally and is considered to be too insignificant relative to the high uncertainty in estimating it to be considered in the model.

The Acy_{Relev} model can be taken one step further by performing multiple linear regression on the five acid relevant species. The primary purpose of performing the regression is to assess the validity of the included species and consider contributions other than 100% for each species. Multiple linear regression of the measured acidity against the five acid relevant species produces the following equation:

$$[Acy_{Regress}] = 0.56 + 0.83[nss SO_4^{2-}] + 0.95[NO_3^-] + 1.44[excess Cl^-] - 0.97[excess NH_4^+] - 1.00[nss Ca^{2+}] \quad (10)$$

All coefficients in the regression equation are significantly different from zero with $p < 0.001$. This model explains 86.8% of the variance in the measured data, which equates to a correlation coefficient of 0.931, only slightly better than the Acy_{Relev} model. The regression coefficients provide good agreement with the assumptions that nearly all of the ammonium is derived from ammonia, nearly all of the non sea salt calcium is derived from calcium carbonate, and nearly all of the nitrate is derived from HNO_3 . The coefficients also suggest an underestimation of HCl and an overestimation of the amount of acidic sulfate, while the y-intercept value suggests that perhaps there are some additional acids that have not been accounted for. These additional acids could be organic acids, since the y-intercept of 0.53 is roughly the same magnitude as the mean

organic acid anion concentrations of 0.3 – 0.4 μeq reported for ice cores from Summit, Greenland (*Legrand and De Angelis, 1996*).

These coefficients must be interpreted with caution, however, because they do not necessarily reflect the true proportion of acidity contributed by each species. The regression model assumes that all of the error is normally distributed error in the measured acidity, when in fact there is error of comparable magnitude in each of the acid species. The error in the measured acidity may be non-normal, and instead biased positively during troughs and negatively during peaks due to signal smoothing, particularly during the highest amplitude events that weight the regression more heavily. There is also likely to be seasonal or long term variation in the proportion of each species affecting the acidity measurement, which will not be accounted for in the linear regression model, and the absence of organic acids will affect the model coefficients.

Despite these caveats, it is interesting to consider the model, as a means of assessing possible deficiencies in the $\text{Acy}_{\text{Relev}}$ model. It is difficult to account for the approximate 17% of the sulfur that is suggested to be non-acidic by the regression model, since MSA is expected to account for less than 3% of the sulfur acidity during the time frame of the Humboldt North record. Calcium sulfate should be accounted for by the subtraction of calcium equivalents in Equation 9, and should not require specific consideration, however a SO_4/Ca molar ratio of 0.075 to account for Gypsum sulfate in Greenland ice cores (*Patris et. al, 2002*) indicates that an average of about 2% of the Sulfate is derived from non non-acidic dust sources. Additional sources of non-acidic sulfur or a loss mechanism other than HCl reemission are possible explanations. The results of the regression model are also consistent with a reduction in amplitude of the

measured acidity due to signal smoothing, and it is likely that this accounts for some of the reduced sulfur coefficient and the intercept term. A representative portion of the time series of the Acy_{Regres} , Acy_{Relev} and Acy_{IonBal} models along with the measured acidity are presented below in Figure 4.

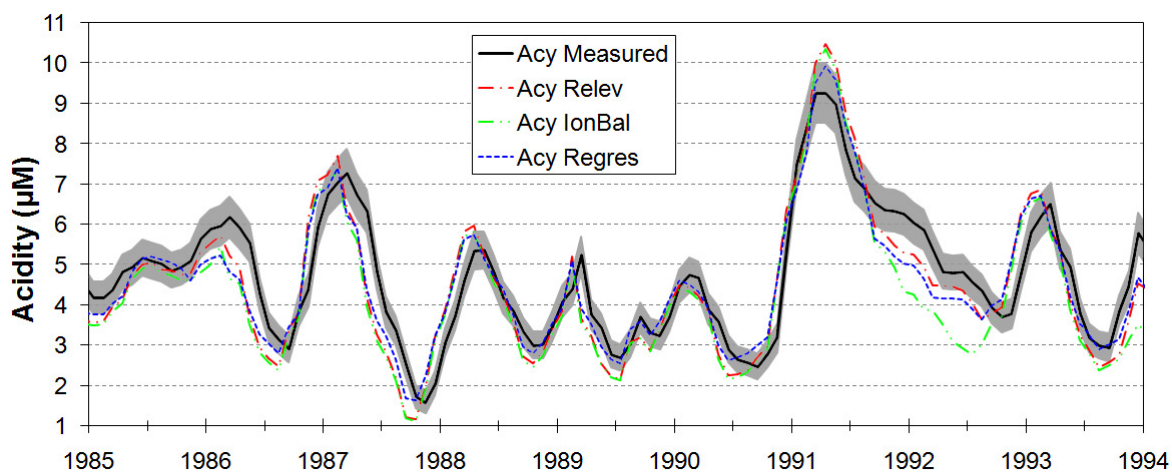


Figure 4 A comparison of the various modeled versions with the measured acidity for a representative portion of the time series. The shaded area is the 95% confidence interval of the acidity measurement. The ion balance model is subject to the greatest error because it incorporates all species in the sample. The relevant species model performs better because it includes only the five species expected to be driving the acidity, and the regression model provides the best fit using the five acid relevant species.

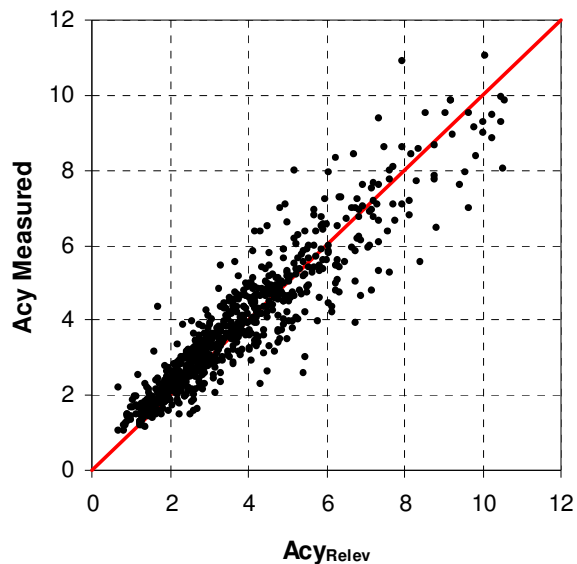


Figure 5 Scatter plot of measured vs. Acy_{Relev} modeled data showing a near 1-1 correlation with an even distribution of error. The model underestimation of the lowest values can be seen in the lower left of the diagram.

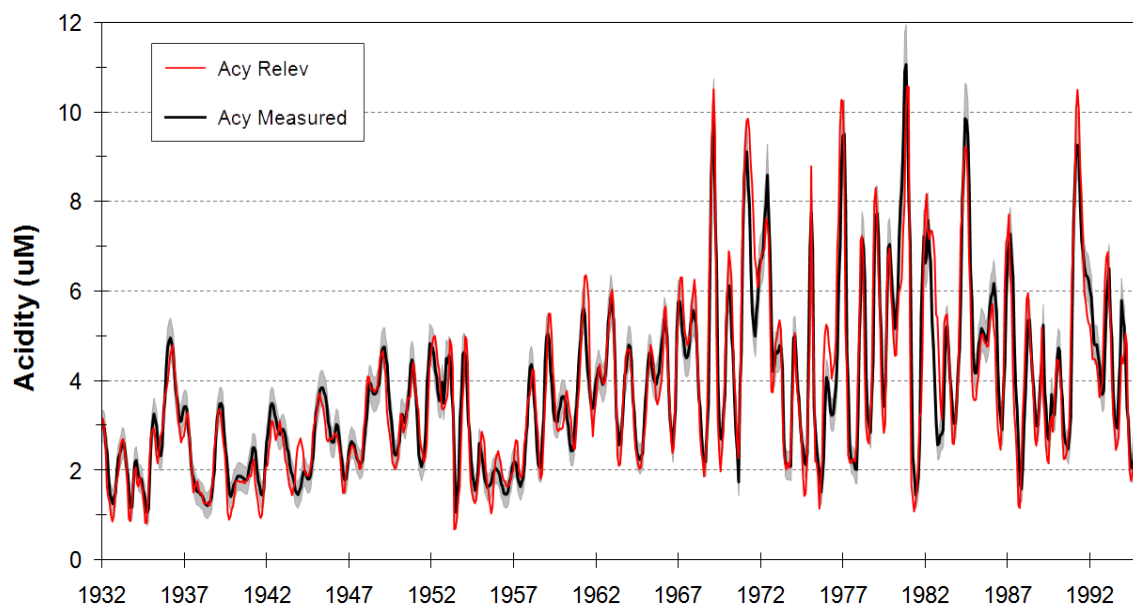


Figure 6 Comparison of Acy_{Relev} with the measured acidity profile. The shaded area is the 95% confidence interval of the measured data. The slight overestimation of peaks and underestimation of troughs is evident.

Excess Chloride

Excess chloride plays a minor, but significant role in determining the acidity of the ice core. It is assumed to represent HCl, with sources including sea salt dechlorination by acid displacement, volcanic emissions, biomass burning, coal combustion, and waste incineration, with the majority attributed to sea salt dechlorination by acid displacement (*Legrand et al.*, 2002; *Keene et al.*, 1999). Considerable uncertainty regarding the mechanisms of sea salt dechlorination exist, however (*Keene et al.*, 1999; *Erickson 1999*). While *Legrand et al.* (2002) found an increase in excess chloride coinciding with a general increase in acidity at Summit, Greenland and concluded that increased sea salt dechlorination was due to increased total acidity, our record shows excess chloride concentrations remaining steady until the 1960s before increasing, coinciding more closely with the increase in nitrate concentration than with sulfate or acidity in general (Figure 8). This timing suggests that total acidity alone is not the only relevant factor, and that anthropogenic HNO₃ may be responsible for a significant increase in atmospheric HCl over the last 50 years. The apparent role of nitrate in excess chloride formation is supported by aerosol studies that have found nitrate to dominate the chloride depletion of sea salt aerosols (*Zhao and Gao*, 2008).

During most of the record the values of excess chloride are small and do not exert a strong impact on $A_{cy_{Relev}}$, however there are a few instances where significant events occur. Figure 7 shows an acid peak in ~May, 1972 that would go unexplained without consideration of excess chloride. This acidity peak, driven by an excess chloride concentration of ~1.4 μM , is unique in the Humboldt North record, and may represent a unique pollution event or a volcanic eruption. Volcanic HCl can result from either direct

emission or enhanced sea salt dechlorination by acid displacement (*Keene et al.*, 1999). Other distinct excess chloride peaks occur in the winter-spring of 1936 ($0.7 \mu\text{M}$) and 1991 ($1.0 \mu\text{M}$).

It is possible that the 1991 peak represents stratospheric fallout from the 1991 eruption of Mt. Pinatubo, however the emissions from this tropical eruption would not have likely reached the arctic so soon (*Zeilinski et al.*, 1994). There are no very large volcanic eruptions that can clearly explain these excess chloride peak in 1936. Due to the ± 1 year accuracy of the dating and a 1 to 2 year travel time for emissions that reach the stratosphere it is difficult to do anything more than speculate about which moderate Northern Hemisphere eruptions may have had an influence around the time of excess chloride peaks. Without a mechanism beyond eruption timing to distinguish between volcanic and industrial emissions, the origin of the distinct excess chloride peaks remains unclear.

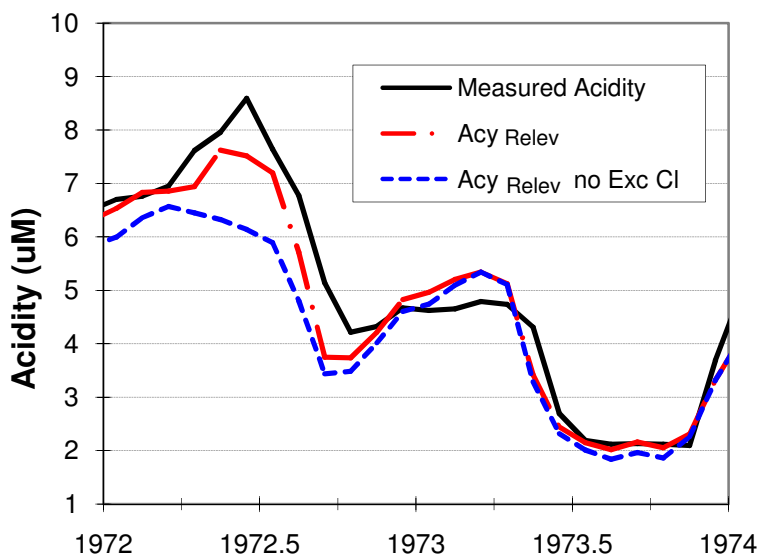


Figure 7 An acidity spike of $1.5 \mu\text{M}$ in mid 1972 (± 1 year) that is driven entirely by excess chloride, or HCl. This type of event is unique in the 63 year record and may be the result of volcanism.

Recent Trends

With the $\text{Acy}_{\text{Relev}}$ model providing a reasonable estimate of the species driving the acidity of the ice core record, the time series of each species concentration provides insight into why the acidity has changed over time. Figure 8 shows the 10-year moving averages of the five primary species measured in units of $\mu\text{eq/L}$. Non sea salt sulfate, the primary driver of acidity, begins the record with only a slightly higher concentration than nitrate, but proceeds to rise dramatically to exert an influence approximately double that of nitrate in the 1960s. The sulfate concentration peaks around 1970, then slowly declines toward the end of the record. Meanwhile, nitrate increases during the period of sulfate decline. Excess chloride increases by a factor of 3 from about 1960 onward, correlating closely with the increasing trend in nitrate. The excess ammonium concentration shows some variation, but displays no clear trend during the record, while calcium varies little throughout the record. Taken together, the trends in the individual chemical species reveal a pre-1965 rise in acidity due primarily to increased H_2SO_4 , then a subsequent stabilization where the decreasing H_2SO_4 was balanced by increasing HNO_3 and HCl .

The peak in sulfur concentration occurring around 1970 is earlier than the estimated emissions peaks of the USA, the former Soviet Union, and all major sulfur emitting countries of Europe, except for the United Kingdom, which peaked in the 1950s, and Germany, which plateaued beginning in the 1960s (*Lefohn et al*, 1999). No significant decrease in transport from mid-latitudes since 1970 is expected because the North Atlantic Oscillation (NAO) shifted from negative to positive at this time, which would only be expected to increase mid-latitude transport, not decrease it (*Eckhardt et*

al., 2003). This early peak in sulfur concentrations may be indicative of the significant role that western European emissions are believed to play in the transport of pollution to the arctic (*Klonecki et al*, 1993), however caution must be applied when assessing the sulfur trend since it represents both anthropogenic and volcanic emissions. It is possible that volcanism in the late 1960s and 1970 contributed to the 1970 peak in the sulfur trend.

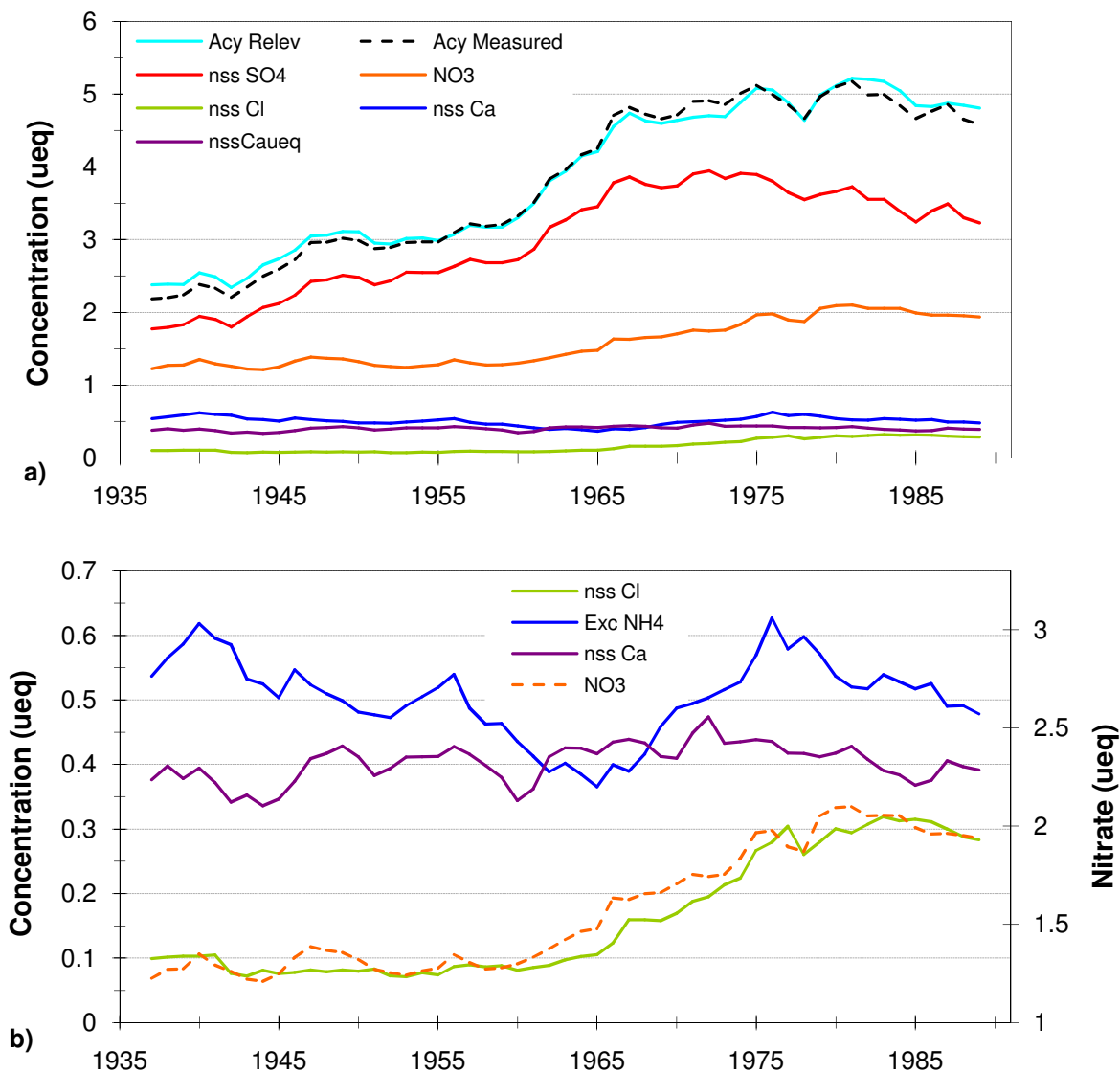


Figure 8 a) 10-year average of measured acid relevant species concentrations in the Humboldt North ice core. b) Same as 7a, but rescaled to show low concentration species. The nitrate trend is plotted as a dashed line with units on a secondary axis, and serves to demonstrating the similarity with the chloride trend.

At an altitude of 1,905 meters and a latitude of 78.5° N, it is likely that the Humboldt North site is receiving chemical inputs from Arctic Haze, of which H⁺ ion from sulfuric acid is a significant component (*Quinn et al.*, 2007). Comparison of aerosol H⁺ concentration measured at Alert, Canada and our measured acidity data shows similar downward trends in both records (Figure 9). The Humboldt North site is located 450 km southeast of Alert and 1,700 meters higher in elevation. The period of overlap in the two records is 14 years (1981 – 1994). While there is disagreement in specific years, the similar downward trend in each record suggests that the two records may be recording the decrease in Arctic Haze that has occurred with recent emissions reductions. This apparent agreement between the two records suggests that earlier portions of the ice core record may also be representative of trends in Arctic Haze, however, the short period of overlap in the two records makes it difficult to draw too many conclusions from the observed similarities. An updated ice core from the Humboldt site would double the period of instrumental overlap and significantly enhance the comparison with the Alert data.

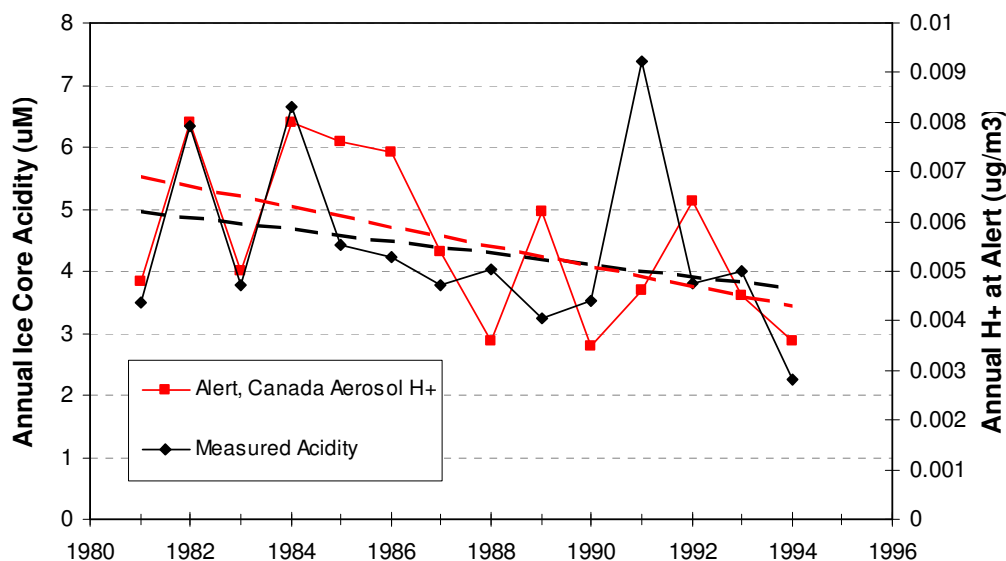


Figure 9 Time series of annual measured acidity in the Humboldt North ice core and annual aerosol H⁺ concentration at Alert, Canada. The dashed lines are linear trends over the 14 year time period. Both records share a similar downward trend, suggesting that the Humboldt ice core may be recording trends in Arctic Haze.

Summary and Future Research

The continuous measurement of ice core acidity has been accomplished through the use of a traditional glass pH electrode and a carbon dioxide equilibration chamber. Electrode calibration is performed with acidity standards rather than pH buffers for maximum accuracy, and Acidity is calculated from the calibrated pH measurement using the constant carbon dioxide concentration. The standard error of annual values, for which the effects of signal smoothing are negligible, is < 0.2 µM between 0 and 5 µM, and < 5% above 5 µM. Signal smoothing due to mixing in the carbon dioxide bubbling chamber can create a small negative bias during high-amplitude seasonal peaks and a small positive bias on high-amplitude seasonal troughs.

The method was applied to the 63-year Humboldt North ice core from northwest Greenland. Comparison of the acidity time series with simultaneous measurements of

major ions has allowed for clear determination of the acid relevant species. It has been estimated that nearly all of the nitrate, ammonium and non sea salt calcium drive the acidity as nitric acid, ammonia, and calcium carbonate, respectively. It is apparent that less than 100% of the sulfur is driving the acidity as sulfuric acid in the Humboldt North record, and although it is almost certainly greater than 80%, the exact proportion is uncertain. Other sources of sulfur include mineral dust and methanesulfonic acid, a monoprotic acid. Excess chloride provides additional acidity, and the timing of its increase in the mid 20th century coincides closely with the increase in nitrate concentrations. This timing supports existing evidence that sea salt aerosol dechlorination by acid displacement occurs more readily in the presence of nitric acid, and suggests that anthropogenic nitrate contamination may be responsible for a significant increase in atmospheric HCl since 1960.

Future research into the species contributions to acidity will benefit from measurements of methanesulfonic acid (MSA), the organic acid anions formate and acetate, and fluoride. All of the significant atmospheric acids and bases would then be accounted for and uncertainty in the acid contribution of each species will be reduced. Excess fluoride is sometimes present in volcanic plumes as hydrofluoric acid, and is an acid which can also serve as a potential volcanic tracer (*Preunkert et al.*, 2001). Work toward establishing additional volcanic tracers would be helpful for separating the anthropogenic from volcanic sulfur emissions.

Recent trends in the relevant species show that reductions in SO₂ emissions, the precursor to H₂SO₄, have led to a reduction in acid deposition. However, these decreases have been partially offset by increases in HNO₃ and HCl. The HNO₃ increase is

presumed to be the result of increases in the NO_x precursors, which are emitted in large part by electrical power utilities and automobile exhaust. The source of the HCl may be partly due to direct industrial emissions, but existing research suggests it is mostly the result of increased acid displacement of HCl on sea salt aerosols (*Keene et al.*, 1999).

The ice core acidity shares a common downward trend with aerosol H⁺ concentrations from Alert, Canada, during the 14 years of overlap in the two records. The common trend may be due to both sites recording the same decrease in the Arctic Haze. If the winter-spring chemical concentrations recorded in the Humboldt core are primarily derived from Arctic Haze, then ice cores from the Humboldt site will provide a long term proxy for the extent and composition of the haze. An updated ice core from the Humboldt site will double the period of overlap with Alert aerosol data and allow for stronger conclusions to be drawn regarding Arctic Haze constituents in ice cores from the Humboldt site.

References

- Anklin, M., R. C. Bales, E. Mosley-Thompson, K. Steffen, Annual accumulation at two sites in northwest Greenland during recent centuries, *J Geophys. Res.*, 103, D22, 28,775-28,783, 1998.
- Barrie, L. A., Arctic air pollution: an overview of current knowledge, *Atmospheric Environment*, 20, 4, 643-663, 1986.
- Drever, J. I., D. R. Hurcomb, Neutralization of atmospheric acidity by chemical weathering in an alpine drainage basin in the north cascade mountains, *Geology*, 14, 3, 221-224, 1986.
- Eckhardt S., A. Stohl, S. Beirle, N. Spichtinger, P. James, C. Forster, C. Junker, T. Wagner, U. Platt, and S. G. Jennings, The North Atlantic Oscillation controls air pollution transport to the Arctic, *Atmos. Chem. Phys.*, 1769–1778, 2003.
- Erickson, D. J. III, C. Seuzaret, W. C. Keene, and S. L. Gong, A general circulation model based calculation of HCl and ClNO₂ production from sea salt dechlorination: Reactive Chlorine Emissions Inventory, *J. Geophys. Res.*, 104, D7, 8347-8372, 1999.
- Ginot P., C Kull, M. Schwikowski, U. Schotterer, H. W. Gaggeler, Effects of postdepositional processes on snow composition of a subtropical glacier (Cerro Tapado, Chilean Andes), *J. Geophys Res.*, 106, D23, 32375-32386, 2001.
- Girard, E., J. P. Blanchet, and Y. Dubois, Effects of arctic sulphuric acid aerosols on wintertime low level atmospheric ice crystals, humidity and temperature at Alert, Nunavut, *Atmospheric Research*, 73, 1-2, 131-148, 2005.
- Hammer, C.U., Initial direct current in the buildup of space charges and the acidity of ice cores. *J. Phys Chem.*, 87, 21, 4099-4103, 1983.
- Isaksson E., V. Pohjola, T. Jauhianinen, J. Moore, J. M. Pinglot, R. Vaikmae, R. S. W. van de Wal, J. O. Hagen, J. Ivask, L. Karlof, T. Martma, H.A.J. Meijer, R. Mulvaney, M. Thomassen, M. van den Broeke, A new ice-core record from Lomonosovfonna, Svalbard: viewing the 1920-97 data in relation to present climate and environmental conditions, *J. Glaciology*, 47, 157, 335-345, 2001.
- Jang, M., N. M. Czoschke, S. Lee, R. M. Kamens, Heterogeneous atmospheric aerosol production by acid-catalyzed particle-phase reactions, *Science*, 298, 814–817, 2002.
- Johnson D. W., J. Turner, J.M. Kelly, The effects of acid rain on forest nutrient status, *Water Resources Research*, 18, 3, 449-461, 1982.
- Keene, W. C., M. A. K. Khalil, D. J. Erickson III, A. Mculloch, T. E. Graedel, J. M. Lobert, M. L. Aucott, S. L. Gong, D. B. Harper, G. Kleiman, P. Midgley, R. M.

- Moore, C. Seuzaret, W. T. Sturges, C. M. Benkovitz, V. Koropalov, L. A. Barrie, and Y. F. Li, Composite global emissions of reactive chlorine from anthropogenic and natural sources: Reactive Chlorine Emissions Inventory, *J. Geophys. Res.*, 104, D7, 8249-8440, 1999.
- Killawee, J. A., I. J. Fairchild, J.-L. Tison, L. Janssens, R. Lorrain, Segregation of solutes and gases in experimental freezing of dilute solutions: Implications for natural glacial systems, *Geochim. et Cosmo. Acta*, 62, 23/24, 3637-3655, 1998.
- Klonecki, A., P. Hess, L. Emmons, L. Smith, J. Orlando, and D. Blake, Seasonal changes in the transport of pollutants into the Arctic troposphere-model study, *J. Geophys. Res.*, 108, D4, 8367, 2003.
- Lefohn A. S., J. D. Husar, and R. B. Husar, Estimating Historical Anthropogenic Global Sulfur Emission Patterns for the Period 1850-1990, *Atmospheric Environment*, 33, 21, 3435-3444, 1999.
- Legrand, M. R., A. J. Aristarain, and R. J. Delmas, Acid Titration of Polar Snow, *Anal. Chem.*, 54, 1336-1339, 1982.
- Legrand M. and M. De Angelis, Light carboxylic acids in Greenland ice: A record of past forest fires and vegetation emissions from the boreal zone, *J. Geophys. Res.*, 101, D2, 4129-4145, 1996.
- Legrand, M. Sulfur-containing species (methanesulfonate and SO₄) over the last climatic cycle in the Greenland Ice Core Project (central Greenland) ice core, *J. Geophys. Res.*, 102, C12, 26,663–26,679, 1997.
- Legrand, M., S. Preunkert, D. Wagenbach, and H. Fischer, Seasonally resolved Alpine and Greenland ice core records of anthropogenic HCl emissions over the 20th century, *J. Geophys. Res.*, 107, D12, 4193, 2002.
- Likens, G. E., R. F. Wright, J. N. Galloway and T. J. Butler, Acid rain, *Sci. Amer.*, 241, 4, 43-51, 1979.
- Likens, G.E., C. T. Driscoll, D. C. Buso, Long-Term Effects of Acid Rain: Response and Recovery of a Forest Ecosystem, *Science*, 272, 5259, 244-246, 1996.
- Maupetit, F. and R. J. Delmas, Carboxylic acids in high-elevation alpine glacier snow, *J. Geophys. Res.*, 99, D8, 16,491–16,500, 1994.
- McConnell, J. R., G. W. Lamorey, S. W. Lambert, and K. C. Taylor, Continuous chemical analyses using inductively coupled plasma mass spectrometry, *Env. Sci. and Tech.*, 36, 2002.
- Moore, J. C., E. W. Wolff, H. B. Clausen, and C. U. Hammer, The Chemical Basis for the Electrical Stratigraphy of Ice, *J. Geophys. Res.*, 97, B2, 1887-1896, 1992.

- Moore, J. C., E. W. Wolff, H. B. Clausen, C.U. Hammer, M. Legrand, K. Fuhrer, Electrical response of the Summit-Greenland ice core to ammonium, sulphuric acid, and hydrochloric acid, *Geophys. Res. Lett.*, 21, 7, 565-568, 1994.
- Neftel, A, H. Oeschger, J. Schwander, and B. Stauffer, Carbon dioxide concentration in bubbles of natural cold ice, *J. Phys. Chem.*, 87, 21, 4116-4120, 1983.
- Oden S., The Acidification of the Atmosphere and Precipitation and its Consequences in the Natural Environment, Swedish National Science Research Council, Bulletin 1, Stockholm, 1968.
- Patris, N., R. J. Delmas, M. Legrand, M. De Angelis, F. Ferron, M. Stievenard, and J. Jouzel, First sulfur isotope measurements in central Greenland ice cores along the preindustrial and industrial periods, *J. Geophys. Res.*, 107, D11, 4115, 2002.
- Preunkurt, S., M. Legrand, and D. Wagenbach, Causes of enhanced fluoride levels in Alpine ice cores over the last 75 years: Implications for the atmospheric fluoride budget, *J. Geophys. Res.*, 106, D12, 12,619-12,6132, 2001.
- Quinn, P. K., G. Shaw, E. Andrews, E. G. Dutton, T. Ruoho-Airola, and S. Gong, Arctic Haze: current trends and knowledge gaps, *Tellus*, 59B, 99-114, 2007.
- Schindler D. W., Effects of acid rain on fresh water ecosystems, *Science*, 239, 4836, 149-157, 1988.
- Simoes, J. C. and V. S. Zagorodnov, The record of anthropogenic pollution in snow and ice in Svalbard, Norway, *Atmos. Env.*, 35, 2, 403-413, 2001.
- Stumm, W., and J. J. Morgan, Aquatic Chemistry, 3rd Edition, Wiley-Interscience, New York, 1995, 1040p.
- Walker T. R. S. D. Young, P.D. Crittenden, and H. Zhang, Anthropogenic enrichment of snow and soil in north-eastern European Russia, *Env. Pollution*, 121, 1, 11-21, 2003
- Wolff E. W., J. C. Moore, H. B. Clausen, and C. U. Hammer, Climatic implications of background acidity and other chemistry derived from electrical studies of the Greenland Ice Core Project ice core, *J. Geophys. Res.*, 102, C12, 26,325-26,332, 1997a.
- Wolff E. W., W.D. Miners, J. C. Moore, and J. G. Paren, Factors Controlling the Electrical Conductivity of Ice from the Polar Regions – A Summary, *J. Phys. Chem. B*, 101, 6090-6094, 1997b.
- Zhao, Y. and Y. Gao, Acid species and chloride depletion in coarse aerosol particles in the US east coast, *Sci. of the Total Env.*, 407, 541-547, 2008.

Zielinski, G. A., P. A. Mayewski, L. D. Meeker, S. Whitlow, M. S. Twicker, M. Morrison, D. A. Meese, A. J. Gow, R. B. Alley, Record of Volcanism Since 7000 B.C. from the GISP2 Greenland Ice Core and Implications for the Volcano-Climate System, *Science*, 264, 5161, 948-952, 1994.